arXiv:hep-ph/0109279v3 9 Jan 2002

Exact Differential $\mathcal{O}(\alpha^2)$ Results for Hard Bremsstrahlung in e^+e^- Annihilation to Two Fermions At and Beyond LEP2 Energies [*]

S. Jadach[†]
CERN, Geneva 23, Switzerland,
M. Melles,
Paul-Scherrer-Institut, Wurenlingen und Villigen, Switzerland,
B.F.L. Ward[‡]
Werner-Heisenberg-Institut, Max-Planck-Institut fur Phyzik, Munich, Germany
S. A. Yost
Department of Physics and Astronomy, University of Tennessee,
Knoxville, Tennessee 37996-1200, USA

July 2001

MPI-PhT-2001-22, UTHEP-01-0701

Abstract

We present the exact $\mathcal{O}(\alpha)$ correction to the process $e^+e^- \to f\bar{f} + \gamma$, $f \neq e$, for ISR⊕FSR at and beyond LEP2 energies. We give explicit formulas for the completely differential cross section. As an important application, we compute the size of the respective sub-leading corrections of $\mathcal{O}(\alpha L)$ to the $f\bar{f}$ cross section, where L is the respective big logarithm in the renormalization group sense so that it is identifiable as $L = \ln|s|/m_e^2$ when s is the squared e^+e^- cms energy. Comparisons are made with the available literature. We show explicitly that our results have the correct infrared limit, as a cross-check. Some comments are made about the implementation of our results in the framework of the Monte Carlo event generator $\mathcal{KK}$ MC.

---

[*] Work supported in part by the US DoE, contract DE-FG05-91ER40627, by the Polish Government, grants KBN 2P03B08414 and KBN 2P03B14715, and by the US-Poland Maria Sklodowska-Curie Fund II PAA/DOE-97-316.

[†] Permanent address: Institute of Nuclear Physics, ul. Kawiory 26a, PL 30-059 Cracow, Poland

[‡] Permanent Address: Department of Physics and Astronomy, University of Tennessee, Knoxville, TN 37996-1200, USA

Currently, the final LEP2 data analysis is in its beginning stages, and the desired total precision tags on the important LEP2 physics processes $e^+e^- \to f\bar{f}$, $f \neq e$, are already called out in the LEP2 MC Workshop in Ref. [1]. It has been demonstrated in Ref. [1] that the Monte Carlo (MC) event generator program $\mathcal{KK}$ [2], hereafter referred to as $\mathcal{KK}$ MC , and the semi-analytical program ZFITTER [3] realize these precisions $(.2 - 1\%)$ in most channels for inclusive cross sections and that for the fully differential distributions, the $\mathcal{KK}$ MC again meets most of the requirements for the LEP2 final data analysis. In this paper, we present exact results on the $\mathcal{O}(\alpha)$ correction to the single hard bremsstrahlung processes $e^+e^- \to f\bar{f} + \gamma$, $f \neq e$. This correction is an important contribution to the differential distributions as they are realized in the $\mathcal{KK}$ MC which allows the very demanding precisions just cited to be achieved.

Specifically, the exact results for the $\mathcal{O}(\alpha)$ corrections to s-channel annihilation hard bremsstrahlung processes under study here were also considered in Refs. [4,5]. We differ from these results as follows. Concerning Ref. [4], the entire result was given only for the case in which the photon angle variables are all integrated out; here, we give the fully differential results. With regard to Ref. [5], the completely differential results were given as well but the mass corrections were omitted. In our work, the masses of the electrons and positrons and the masses of the final state fermion and anti-fermion are exactly taken into account in contrast to the literature. Thus, by comparing with the two calculations in Refs. [4,5] as we do here, we get a measure of the size of the mass corrections as well as cross checks on both our differential and our integrated results.

Our work is organized as follows. In Section 1, we set our notational conventions. In Section 2, we present our exact amplitudes for the $\mathcal{O}(\alpha)$ virtual corrections to initial-state and final-state real radiation. In Section 3, we derive the differential cross-sections corresponding to these amplitudes in a form useful for comparisons. In Section 4, we compare these results with those in Refs. [4,5] while illustrating our results as they are used in the $\mathcal{KK}$ MC in Ref. [2]. Section 5 contains our summary remarks. The Appendix contains technical details about the scalar integrals.

1 Preliminaries

In this section we set our notational conventions. We will use the conventions of Refs. [2,6,7] for our spinors. These conventions are based on the Kleiss-Stirling [8] Weyl spinors augmented as described in Refs. [2,6,7] with the rules for controlling their complex phases, or equivalently, the three axes of the fermion rest frame in which the spin of that fermion is quantized. We sometimes refer to this fermion rest frame as the global positioning of spin

(GPS) frame and to the rule for determining it as the GPS rule. The resulting conventions for the fermion spinors are then called the GPS spinor conventions. See Refs. [2,6,7] for more details. Let us now turn to the kinematics.

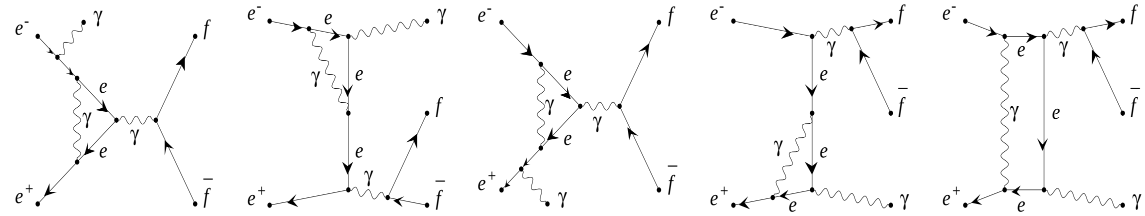

Figure 1: Representative initial state radiation graphs for $e^+e^- \to f\overline{f}$ with one virtual and one real photon, for $f \neq e$.

The process under discussion here is shown in Fig. 1, the one-loop virtual correction to the hard bremsstrahlung process $e^-e^+ \to f\bar{f}+\gamma$, for $f \neq e$. We will treat both the initial state radiation (ISR) case and the final state radiation (FSR) case. We denote the four momenta and helicity of the e^-, e^+, f, and $\bar{f}$ as p_j and λ_j, $j = 1, ..., 4$, respectively. We denote the charge of f by Q_f in units of the positron charge e. The rest mass of fermion f is denoted by m_f. The photon momentum and helicity will be denoted by k and σ. With our GPS conventions for spinors, we induce the following polarization vectors for photons:

$$(\epsilon^\mu_\sigma(\beta))^* = \frac{\bar{u}_\sigma(k)\gamma^\mu u_\sigma(\beta)}{\sqrt{2}\,\bar{u}_{-\sigma}(k)u_\sigma(\beta)}, \quad (\epsilon^\mu_\sigma(\zeta))^* = \frac{\bar{u}_\sigma(k)\gamma^\mu \mathfrak{u}_\sigma(\zeta)}{\sqrt{2}\,\bar{u}_{-\sigma}(k)\mathfrak{u}_\sigma(\zeta)}, \tag{1.1}$$

where the auxiliary 4-vector β is exploited here to simplify our expressions as needed. It satisfies $\beta^2 = 0$. The second choice with $\mathfrak{u}_\sigma(\zeta)$, as defined in Ref. [2], is already an example of this exploitation – it often leads to simplifications in the resulting photon emission amplitudes.

The calculations which we present have been done using the program FORM of Ref. [9]. For the t-channel case, we presented similar results in Ref. [10] in connection with the respective $\mathcal{O}(\alpha^2)L$ corrections needed for the 0.061% (0.054%) total precision tag achieved in Ref. [11] for the LEP1/SLC luminosity process in the Monte Carlo event generator BHLUMI4.04 in Ref. [12]. Just as in the latter case, here a considerable effort is needed to simplify our initial raw FORM output in order to make a practical application of the respective results in the context of a Monte Carlo environment such as the $\mathcal{KK}$ MC in Ref. [2]. As in Ref. [10], we only present the final simplified expressions in this paper for the sake of clarity.

Our metric is that of Bjorken and Drell in Ref. [13] and we effect our gauge invariant calculation in the 't Hooft-Feynman gauge. With these preliminary remarks, we turn now in the next section to the calculation of our process of interest.

2 Exact Results on the Virtual Correction to $e^+e^- \to f\bar{f} + \gamma$, $f \neq e$

In this section we calculate the exact virtual correction to $e^+e^- \to f\bar{f} + \gamma$, $f \neq e$. We proceed in analogy with our results on the virtual correction for the t-channel dominated low angle Bhabha scattering process with a single hard bremsstrahlung in Ref. [10].

Specifically, we express the exact amplitude for one real and one virtual photon emitted from the electron lines in the process $e^+e^- \to f\bar{f} + \gamma$ using the GPS conventions [2,6,7]. In Ref. [10], the corresponding t channel result was obtained for electron line emission. Here, from the latter result, we first obtain the respective initial-state s channel result by crossing the outgoing electron line with the incoming positron line, and replacing the respective final state by $f\bar{f}$, while adding also Z boson exchange. The results are translated into GPS conventions. Then, in subsection 2.2, we provide the detailed form factors appearing in the initial state amplitudes. The corresponding final state amplitudes are presented in subsections 2.3 and 2.4.

2.1 ISR s-Channel Exact Result

In this subsection, we define notation and set up the exact contribution for one real photon and one virtual photon emitted from the electron lines in the process $e^+e^- \to f\bar{f} + \gamma$. The amplitude for real plus virtual photon emission from the initial state may be written

$$\mathcal{M}_1^{\mathrm{ISR}(1)} = \frac{Q_e^2 e^2}{16\pi^2} \mathcal{M}_1^{\mathrm{ISR}(0)} \left(f_0 + f_1 I_1 + f_2 I_2 \right) , \tag{2.1}$$

where the real photon emission amplitude is $\mathcal{M}_1^{\mathrm{ISR}(0)}$, and the factors $I_{0,1,2}$ contain spinor dependence. They will be specified in the next section.

In GPS conventions, the amplitude $\mathcal{M}_1^{\mathrm{ISR}(0)}$ for the initial state radiation of a single photon is given by

$$\begin{aligned} \mathcal{M}_1^{\mathrm{ISR}(0)} \begin{bmatrix} p \\ \lambda \end{bmatrix} &= \frac{eQ_e}{2kp_1} \overline{v}(p_2, \lambda_2) \mathbf{M}_1 (\not{p}_1 + m - \not{k}) \not{\epsilon}_\sigma^\star u(p_1, \lambda_1) \\ &+ \frac{eQ_e}{2kp_2} \overline{v}(p_2, \lambda_2) \not{\epsilon}_\sigma^\star (-\not{p}_2 + m + \not{k}) \mathbf{M}_1 u(p_1, \lambda_1) , \end{aligned} \tag{2.2}$$

where

$$\mathbf{M}_1 = ie^2 Q_f \sum_{\substack{B=\gamma,Z \\ \lambda,\mu=\pm 1}} \left(\frac{\overline{u}(p_3, \lambda_3) \gamma_\sigma g_\lambda^{f,B} \omega_\lambda v(p_4, \lambda_4)}{s' - M_B^2 + i\Gamma_B s'/M_B} \right) \gamma^\sigma g_\mu^{e,B} \omega_\mu \tag{2.3}$$

is the annihilation scattering spinor matrix.

The form factors may be obtained from the corresponding t-channel result in Ref. [10] for electron line emission. Specifically, the s channel result can be obtained by crossing the outgoing electron line with the incoming positron line, and replacing the final state by $f\bar{f}$. We also include the effects of Z exchange in the s channel.

Our previous calculations of t-channel bremsstrahlung [10] used the Chinese Magic conventions [14] for the photon polarizations. The GPS version of the magic photon polarization vector is related to the Chinese Magic conventions [14] by

$$\epsilon^{\star \mathrm{GPS}}(k,\beta,\sigma) = \sigma \epsilon^{\mathrm{Chinese}}(k,\beta,-\sigma). \tag{2.4}$$

The purpose of this change is to recover the more standard convention of defining photon polarization in terms of incoming states. The choice of magic polarization vector affects the amplitude (2.1) only through the definition of $\mathcal{M}_1^{\mathrm{ISR}(0)}$. The remaining factors may thus be obtained directly by crossing from our previous t-channel results.

The magic choice of auxiliary vector for initial state radiation is $\beta = h\begin{bmatrix} 0 & p_2 & p_1 \\ \sigma & \lambda_1 & \lambda_2 \end{bmatrix}$, with the definition

$$h\begin{bmatrix} q_0 & q_1 & q_2 \\ \mu_0 & \mu_1 & \mu_2 \end{bmatrix} = \begin{Bmatrix} q_0 \\ q_1 \\ q_2 \end{Bmatrix} \quad \text{if} \quad \left\{ \begin{array}{l} \mu_1 = \mu_2 \\ \mu_0 = \mu_1 = -\mu_2 \\ \mu_0 = \mu_2 = -\mu_1 \end{array} \right. . \tag{2.5}$$

Using the magic polarization vector in (2.1) and neglecting fermion masses gives

$$\mathcal{M}_1^{\mathrm{ISR}(0)} = iQ_e \sigma e^3 G_{\lambda_1,\lambda_3}(s') I_0 \frac{2s_{-\sigma}(p_3,p_4)}{s_\sigma(p_1,k)s_\sigma(p_2,k)}, \tag{2.6}$$

where the photon-Z propagator is

$$G_{\lambda,\mu}(s') = \sum_{B=\gamma,Z} \frac{g_\lambda^{e,B} g_\mu^{f,B}}{s' - M_B^2 + i\Gamma_B s'/M_B}, \tag{2.7}$$

and

$$I_0 = -\sqrt{2}\lambda_1\lambda_3 s_\sigma^2 \left(h\begin{bmatrix} 0 & p_2 & p_1 \\ \sigma & \lambda_1 & \lambda_2 \end{bmatrix}, h\begin{bmatrix} 0 & p_3 & p_4 \\ \sigma & \lambda_3 & \lambda_4 \end{bmatrix} \right). \tag{2.8}$$

We now turn to calculating the form factors and spinor factors.

2.2 Initial State Form Factors

It remains to describe the form factors and spinor factors needed to compute $\mathcal{M}_1^{\mathrm{ISR}(1)}$. The spinor factors $I_{1,2}$ are given by

$$\begin{aligned} I_1 &= \sqrt{2}\lambda_1 s_{-\lambda_1}(p_1,k)s_{\lambda_1}(p_2,k) \\ &\quad \times \frac{s_{-\lambda_1}(p_4,p_1)s_{\lambda_1}(p_1,p_3) - s_{-\lambda_1}(p_4,p_2)s_{\lambda_1}(p_2,p_3)}{s_{-\sigma}(p_1,p_2)s_{-\sigma}(p_3,p_4)s_{-\lambda_1}(p_4,p_2)s_{\lambda_1}(p_2,p_3)I_0}, \qquad (2.9) \\ I_2 &= \frac{\sqrt{2}\sigma s_{-\lambda_1}(p_1,k)s_{\lambda_1}(p_2,k)s_{-\lambda_3}(p_4,k)s_{\lambda_3}(p_3,k)}{s_{-\sigma}(p_1,p_2)s_{-\sigma}(p_4,p_3)I_0} \qquad (2.10) \end{aligned}$$

where the spinor product is $s_\lambda(p,q) = \bar{u}_{-\lambda}(p)u_\lambda(q)$. The factors $I_{1,2}$ are crossed versions of $(\mathcal{I}_1 \pm \mathcal{I}_2)/2\mathcal{I}_0$ in Ref. [10].

We will begin by writing the dominant term f_0. Expressions can be found in Ref. [5] for all of the scalar integrals needed for the form factors, which were previously calculated using the FF package [9], which implements the methods of Ref. [15]. The integrals in Ref. [5] are not quite adequate, because of the possibility that $r_i < m_e^2/s$. However, it was possible to analytically continue when necessary, and to reproduce the numerical results of the FF package. Thus, an expression for the form factors in terms of logarithms and dilogarithms is now available. Details on the s channel version of the scalar integrals used in Ref. [10] may be found in the Appendix.

For $\sigma = \lambda_1$, using $r_i = 2p_i \cdot k/s$,

$$\begin{aligned} f_0 &= 4\pi\, B_{\rm YFS}(s,m_e) + 2\,(L - 1 - i\pi) + \frac{r_2}{1-r_2} \\ &+ \frac{(r_1+r_2)}{(1-r_2)r_1} R(r_1,r_2) + R(r_2,r_1) \\ &+ \left\{3 + \frac{2r_2}{(1-r_2)(r_1+r_2)}\right\} \ln(1-r_1-r_2) \\ &- \frac{r_2(2+r_1)}{(1-r_1)(1-r_2)} \left\{\ln\frac{(1-r_1-r_2)}{r_2} - i\pi\right\} \qquad (2.11) \end{aligned}$$

with $L = \ln(s/m_e^2)$, the infrared YFS factor

$$4\pi\, B_{\rm YFS}(s,m) = \Big(4\ln\frac{m_0}{m} + 1\Big)(\ln\frac{s}{m^2} - 1 - i\pi) - \ln^2(\frac{s}{m^2}) - 1 + \frac{4\pi^2}{3} + i\pi(2\ln\frac{s}{m^2} - 1) \qquad (2.12)$$

and

$$\begin{aligned} R(x,y) &= \ln^2(1-x) + 2\ln(1-x)\left\{\ln\left(\frac{y}{1-x}\right) + i\pi\right\} \\ &+ 2\,{\rm Sp}(x+y) - 2\,{\rm Sp}\left(\frac{y}{1-x}\right) \qquad (2.13) \\ &= \ln^2(1-x) + 2\ln(1-x)\left\{\ln\left(\frac{y}{1-x-y}\right) + i\pi\right\} \\ &+ 2\ln\left(\frac{y}{x+y}\right)\ln\left(\frac{1-x-y}{1-x}\right) - 2\,{\rm Sp}\left(\frac{x}{x+y}\right) \\ &+ 2\,{\rm Sp}(x) + 2\,{\rm Sp}\left(\frac{(1-x-y)x}{(x+y)(1-x)}\right). \qquad (2.14) \end{aligned}$$

The second expression is preferred for calculating $R(x,y)/x$ when x may be small. For $\sigma = -\lambda$, r_1 and r_2 are interchanged in (2.11).

The coefficients of the spinor terms in (2.1) are, for $\sigma = \lambda$,

$$\begin{aligned} f_1 &= \frac{(r_1 - r_2)}{2(1-r_1)(1-r_2)} + \frac{r_2(1-r_1-r_2)}{r_1(1-r_2)(r_1+r_2)} \ln(1-r_1-r_2) \\ &+ \frac{r_1+r_2}{2r_1}\left\{\frac{1-r_1-r_2}{r_1(1-r_2)} + \frac{1}{2}\delta_{\sigma,1}\right\} R(r_1,r_2) + \frac{r_1+r_2}{4r_2}\delta_{\sigma,-1}R(r_2,r_1) \\ &+ \frac{1-r_1-r_2}{(1-r_1)(1-r_2)}\left\{\frac{r_1+r_2}{2(1-r_1)} - \frac{1}{1-r_1} - \frac{r_2}{r_1}\right\} \\ &\qquad \times \left(\ln\frac{1-r_1-r_2}{r_2} - i\pi\right) \end{aligned} \tag{2.15}$$

and

$$\begin{aligned} f_2 &= 2 - \frac{2-r_1-r_2}{2(1-r_1)(1-r_2)} \\ &+ \frac{1-r_1-r_2}{r_1(r_1+r_2)}\left(\frac{2-r_2}{1-r_2}\right)\ln(1-r_1-r_2) \\ &+ \frac{2(1-r_1-r_2)}{r_1+r_2}\left\{1 + \frac{1}{r_1+r_2}\ln(1-r_1-r_2)\right\} \\ &+ \frac{(1-r_1-r_2)(2+r_1-r_2)}{2r_1^2(1-r_2)}R(r_1,r_2) \\ &+ \frac{1}{4}\left(1-\frac{r_2}{r_1}\right)\delta_{\sigma,1}R(r_1,r_2) - \frac{1}{4}\left(1-\frac{r_1}{r_2}\right)\delta_{\sigma,-1}R(r_2,r_1) \\ &- \frac{1-r_1-r_2}{(1-r_1)(1-r_2)}\left(\frac{2-r_2}{r_1} + \frac{r_2-r_1}{2(1-r_1)}\right) \\ &\qquad \times \left(\ln\frac{1-r_1-r_2}{r_2} - i\pi\right). \end{aligned} \tag{2.16}$$

The coefficients $f_{1,2}$ are s-channel versions of $(\mathcal{F}_1 \pm \mathcal{F}_2)/2$ in Ref. [10]. For $\sigma = -\lambda$, r_1 and r_2 are interchanged in (2.15) and (2.16).

The leading log limit is obtained by finding which terms give rise to the leading powers of the 'big logarithm' L when the above expressions are integrated over r_1 and r_2. These come from collinear terms where r_1 or r_2 go to zero. In the collinear limits, when averaged over the azimuthal angle, only the f_0 terms remain to order L^2 and L, *i.e.*, to order NLL. Using the identities

$$\begin{aligned} R(0,y) &= 0, \\ \frac{1}{x}R(x,y) &= 2\left(1-\frac{1}{y}\right)\ln(1-y) - 2\ln y - 2\pi i \text{ for } x \to 0, \\ R(x,y) &= 2\ln(1-x)\left(\ln y + i\pi\right) - \ln^2(1-x) + 2\mathrm{Sp}(x) \text{ for } y \to 0, \end{aligned} \tag{2.17}$$

the NLL limit of the form factor f_0 is found to be

$$\begin{aligned} f_0^{NLL} &= 2(L-1-i\pi)+2\ln(1-r_1)(\ln r_2+i\pi)+2\ln(1-r_2)(\ln r_1+i\pi) \\ &- \ln^2(1-r_1)-\ln^2(1-r_2)+3\ln(1-r_1)+3\ln(1-r_2) \\ &+ 2\,\mathrm{Sp}(r_1)+2\,\mathrm{Sp}(r_2)+\frac{r_1}{1-r_1}\delta_{\sigma,-\lambda_1}+\frac{r_2}{1-r_2}\delta_{\sigma,\lambda_1} \qquad (2.18) \end{aligned}$$

without mass corrections.

Mass corrections we have calculated primarily without any approximations, however, in the following we shall present them in the approximation $m_e << \sqrt{s}$. In particular, in this approximation, we checked by explicit calculation that the result which we obtain for the mass corrections in fact agrees with that implied by the prescription in Ref. [16]. This prescription is valid for the spin-averaged differential distribution in the limit $m_e << \sqrt{s}$, but since mass terms are located in the separate (helicity conservation violating) spin amplitudes, it is not difficult to "undo" the spin summation. The technique of Ref. [16] was originally applied to tree level photon emissions. Following the Appendix B of Ref. [10] we can apply it also to our case of emission of one virtual and one real photon.

Taking advantage of the freedom, which we have for presenting mass terms in the $m_e << \sqrt{s}$ approximation, the introduction of the mass correction leads to a replacement of f_0 by $f_0 + f_0^{m_e}$, where

$$\begin{aligned} f_0^{(m_e)} &= \frac{2{m_e}^2}{s}\left(\frac{r_1}{r_2}+\frac{r_2}{r_1}\right)\frac{(1-r_1)(1-r_2)}{1+(1-r_1-r_2)^2} \\ &\times \{f_0-4\pi\ B_{\mathrm{YFS}}(s',m_e)-2[L+\ln(1-r_1-r_2)-1-i\pi]\} \qquad (2.19) \end{aligned}$$

with YFS infrared factor

$$\begin{aligned} 4\pi\,B_{\mathrm{YFS}}(s',m_e) &= 4\pi\,B_{\mathrm{YFS}}(s,m_e)+\ln(1-r_1-r_2)\ (4\ln\frac{m_0}{m_e} \\ &- 2L+1+2\pi i)-\ln^2(1-r_1-r_2)\ . \qquad (2.20) \end{aligned}$$

Mass corrections first appear at order NLL, and to this order,

$$\begin{aligned} f_0^{(m_e)\ NLL} &= \frac{2{m_e}^2}{s}\left(\frac{r_1}{r_2}+\frac{r_2}{r_1}\right)\frac{(1-r_1)(1-r_2)}{1+(1-r_1-r_2)^2} \\ &\times \Big\{\ln(1-r_1-r_2)\ \left(2L-1-2\pi i-4\ln\frac{m_0}{m_e}\right)+\ln^2(1-r_1-r_2) \\ &+ 2\ln(1-r_1)(\ln r_2+i\pi)+2\ln(1-r_2)(\ln r_1+i\pi)\Big\}. \qquad (2.21) \end{aligned}$$

Only the LL part of f_0 contributes to the mass correction, to order NLL. The result (2.19) gives the complete effect of the mass corrections for the ISR neglecting the terms that are suppressed by higher powers of m_e^2/s as usual.

2.3 Final State Radiation

The amplitudes for final state radiation can be obtained by crossing the incoming electron with the outgoing $\bar{f}$, and the incoming positron with the outgoing f. Thus, $p_1 \leftrightarrow -p_4$, $p_2 \leftrightarrow -p_3$, $\lambda_1 \leftrightarrow -\lambda_4$, and $\lambda_2 \leftrightarrow -\lambda_3$ in the results of the previous sections.

The final state radiation (FSR) amplitude can be written in analogy with the ISR result (2.1),

$$\mathcal{M}_1^{\rm FSR(1)} = \frac{Q_f^2 e^2}{16\pi^2}\mathcal{M}_1^{\rm FSR(0)}\left(\overline{f}_0 + \overline{f}_1\overline{I}_1 + \overline{f}_2\overline{I}_2\right) \tag{2.22}$$

The form factors $\overline{f}_{0,1,2}$ and the spinor factors $\overline{I}_{1,2}$ are final-state analogs of those in the previous section, and will be defined in the next subsection.

The amplitude $\mathcal{M}_1^{\rm FSR(0)}$ for the final state radiation of a single photon can be obtained from the initial state amplitude $\mathcal{M}_1^{\rm ISR(0)}$ by crossing. Crossing leads to spinors with negative energy. A consistent choice of branches gives

$$u(-p,-\lambda) = iv(p,\lambda), \qquad v(-p,-\lambda) = iu(p,\lambda). \tag{2.23}$$

Then we obtain

$$\begin{aligned}\mathcal{M}_1^{\rm FSR(0)}\begin{bmatrix}p\\ \lambda\end{bmatrix} &= \frac{eQ_f}{2kp_4}\overline{u}(p_3,\lambda_3)\overline{\mathbf{M}}_1(\not p_4 - m + \not k)\not\epsilon^\star_\sigma v(p_4,\lambda_4)\\ &- \frac{eQ_f}{2kp_3}\overline{u}(p_3,\lambda_3)\not\epsilon^\star_\sigma(\not p_3 + m + \not k)\overline{\mathbf{M}}_1 v(p_4,\lambda_4),\end{aligned} \tag{2.24}$$

where

$$\overline{\mathbf{M}}_1 = ie^2 Q_e \sum_{\substack{B=\gamma,Z\\ \lambda,\mu=\pm1}}\left(\frac{\overline{v}(p_2,\lambda_2)\gamma_\sigma g_\lambda^{e,B}\omega_\lambda u(p_1,\lambda_1)}{s - M_B^2 + i\Gamma_B s/M_B}\right)\gamma^\sigma g_\mu^{f,B}\omega_\mu. \tag{2.25}$$

The magic polarization vector for final state radiation is $h\begin{bmatrix}0 & p_3 & p_4\\ \sigma & \lambda_3 & \lambda_4\end{bmatrix}$. Using this in (2.24) gives, in the massless limit,

$$\mathcal{M}_1^{\rm FSR(0)} = iQ_f\sigma e^3 G_{-\lambda_4,-\lambda_2}(s) I_0 \frac{2s_{-\sigma}(p_3,p_4)}{s_\sigma(p_1,k)s_\sigma(p_2,k)}, \tag{2.26}$$

with propagator (2.7) and I_0 given again by (2.8).

2.4 Final State Form Factors

The spinor factors $\overline{I}_{1,2}$ appearing in $\mathcal{M}_1^{\rm FSR(1)}$ are given by

$$\begin{aligned}\overline{I}_1 &= \sqrt{2}\lambda_4 s_{\lambda_4}(p_4,k)s_{-\lambda_4}(p_3,k)\\ &\quad\times\frac{s_{\lambda_4}(p_1,p_4)s_{-\lambda_4}(p_2,p_4) + s_{\lambda_4}(p_1,p_3)s_{-\lambda_4}(p_3,p_2)}{s_{-\sigma}(p_4,p_3)s_{-\sigma}(p_2,p_1)s_{\lambda_4}(p_1,p_3)s_{-\lambda_4}(p_3,p_2)I_0},\end{aligned} \tag{2.27}$$

$$\overline{I}_2 = \frac{\sqrt{2}\sigma s_{\lambda_4}(p_4,k)s_{-\lambda_4}(p_3,k)s_{\lambda_2}(p_1,k)s_{-\lambda_2}(p_2,k)}{s_{-\sigma}(p_4,p_3)s_{-\sigma}(p_1,p_2)I_0}. \tag{2.28}$$

As before, let $r_i = 2p_i \cdot k/s$. We can obtain the form factor $\overline{f}_0$ for $\sigma = -\lambda_3$ by substituting

$$r_1 \to -r_3/(1-r_3-r_4), \qquad r_2 \to -r_4/(1-r_3-r_4) \tag{2.29}$$

in (2.11), and for $\sigma = +\lambda_3$ by interchanging r_3 and r_4 in (2.29). (Since $k^2 = 0$, we have $r_1 + r_2 = r_3 + r_4$.) Then, for $\sigma = \lambda_3$,

$$\begin{aligned}
\overline{f}_0 &= 4\pi\, B_{\rm YFS}(s', m_f) + 2\left(L - 2\ln\frac{m_f}{m_e} - 1 - i\pi\right) - \frac{r_3}{1-r_4} \\
&+ \frac{(r_3+r_4)(1-r_3-r_4)}{r_4(1-r_4)}\overline{R}(r_3,r_4) + \overline{R}(r_4,r_3) \\
&- \left\{1 + \frac{2r_3(1-r_3-r_4)}{(1-r_4)(r_3+r_4)}\right\}\ln(1-r_3-r_4) \\
&+ \frac{r_3}{1-r_4}\left\{\frac{3r_4}{1-r_3} - 2\right\}\ln r_3
\end{aligned} \tag{2.30}$$

with

$$\begin{aligned}
\overline{R}(x,y) &= R\left(\frac{-y}{1-x-y}, \frac{-x}{1-x-y}\right) \\
&= 2\ln x \ln\left(\frac{1-x}{1-x-y}\right) + 2\,{\rm Sp}(x) - 2\,{\rm Sp}(x+y).
\end{aligned} \tag{2.31}$$

The expression (2.31) is obtained from (2.13) using the dilogarithm identity

$${\rm Sp}\left(\frac{-x}{1-x}\right) = -{\rm Sp}(x) - \frac{1}{2}\ln^2(1-x). \tag{2.32}$$

The imaginary parts in (2.30) were obtained by assuming the $i\pi$ terms in (2.11) came from a small positive imaginary part on s or s'. For $\sigma = -\lambda_3$, $f_0 = f_0(r_4, r_3)$ instead: r_3 and r_4 are interchanged.

The coefficients of the spinor terms in (2.22) are, for $\sigma = \lambda_3$,

$$\begin{aligned}
\overline{f}_1 &= \frac{(r_3-r_4)(1-r_3-r_4)}{2(1-r_3)(1-r_4)} + \frac{r_3(1-r_3-r_4)}{r_4(1-r_4)(r_3+r_4)}\ln(1-r_3-r_4) \\
&- \frac{r_3+r_4}{2r_4}\left\{\frac{1-r_3-r_4}{r_4(1-r_4)} - \frac{1}{2}\delta_{\sigma,-1}\right\}\overline{R}(r_3,r_4) + \frac{r_3+r_4}{4r_3}\delta_{\sigma,1}\overline{R}(r_4,r_3) \\
&+ \frac{(1-r_3-r_4)}{(1-r_3)(1-r_4)}\left\{1 + \frac{r_3}{r_4} + \frac{r_3-r_4}{2(1-r_3)}\right\}\ln r_3,
\end{aligned} \tag{2.33}$$

$$\overline{f}_2 = 2 - \frac{(1-r_3-r_4)(2-r_3-r_4)}{2(1-r_3)(1-r_4)}$$

$$
\begin{aligned}
&- \frac{1-r_3-r_4}{r_4(r_3+r_4)}\left(2-\frac{r_3}{1-r_4}\right)\ln(1-r_3-r_4) \\
&- \frac{2}{r_3+r_4}\left\{1+\frac{1-r_3-r_4}{r_3+r_4}\ln(1-r_3-r_4)\right\} \\
&+ \frac{(1-r_3-r_4)(2-r_3-3r_4)}{2r_4^2(1-r_4)}\overline{R}(r_3,r_4) \\
&+ \frac{1}{4}\left(1-\frac{r_3}{r_4}\right)\delta_{\sigma,-1}\overline{R}(r_3,r_4)-\frac{1}{4}\left(1-\frac{r_4}{r_3}\right)\delta_{\sigma,1}\overline{R}(r_4,r_3) \\
&- \frac{1-r_3-r_4}{(1-r_3)(1-r_4)}\left\{\frac{2-r_3}{r_4}+\frac{r_4-r_3}{2(1-r_3)}-2\right\}\ln r_3. \qquad (2.34)
\end{aligned}
$$

For $\sigma = -\lambda_3$, r_3 and r_4 are interchanged in (2.33) and (2.34).

The NLL limit is obtained as in the initial state radiation case, except that now the collinear limits are when r_3 or r_4 become small. Only the form factor $\overline{f}_0$ survives to order NLL, and using the identities

$$
\begin{aligned}
\overline{R}(x,0) &= 0, \\
\frac{1}{y}\overline{R}(x,y) &= \frac{2}{1-x}\ln x+\frac{2}{x}\ln(1-x) \text{ for } y\to 0, \\
\overline{R}(x,y) &= -2\ln x\ln(1-y)-2\,\mathrm{Sp}(y) \text{ for } x\to 0, \qquad (2.35)
\end{aligned}
$$

we find

$$
\begin{aligned}
\overline{f}_0^{NLL} &= 4\pi\, B_{\mathrm{YFS}}(s',m_f)+2(L-1-i\pi) \\
&- 2\ln r_3\ln(1-r_4)-2\ln r_4\ln(1-r_3) \\
&- \ln(1-r_3)-\ln(1-r_4)-2\,\mathrm{Sp}(r_3)-2\,\mathrm{Sp}(r_4) \\
&- \delta_{\sigma,\lambda_3}r_3-\delta_{\sigma,-\lambda_3}r_4 \qquad (2.36)
\end{aligned}
$$

without mass corrections.

Spin-averaged mass corrections can be obtained from the initial state case (2.19) by crossing. The result is that $\overline{f}_0 \to \overline{f}_0 + \overline{f}_0^{m_f}$, where

$$
\begin{aligned}
\overline{f}_0^{(m_f)} &= \frac{2m_f^2}{s}\left(\frac{r_3}{r_4}+\frac{r_4}{r_3}\right)\frac{(1-r_3)(1-r_4)}{1+(1-r_3-r_4)^2} \\
&\times \left\{f_0-4\pi\, B_{\mathrm{YFS}f}(s)-2(L-2\ln\frac{m_f}{m_e}-1-i\pi)\right\} \qquad (2.37)
\end{aligned}
$$

where

$$
\begin{aligned}
4\pi\, B_{\mathrm{YFS}f}(s) &= 4\pi\, B_{\mathrm{YFS}}(s',m_f)-\ln(1-r_3-r_4)(4\ln\frac{m_0}{m_e} \\
&- 2L+1+2\pi i)+\ln^2(1-r_3-r_4)\ . \qquad (2.38)
\end{aligned}
$$

Again, mass corrections first appear at order NLL, and to this order,

$$\begin{aligned}
\overline{f}_0^{(m_f)\ NLL} &= -\frac{2m_f^2}{s}\left(\frac{r_3}{r_4}+\frac{r_4}{r_3}\right)\frac{(1-r_3)(1-r_4)}{1+(1-r_3-r_4)^2} \\
&\times \left\{\ln(1-r_3-r_4)\left(4\ln\frac{m_0}{m_f}-2L+4\ln\frac{m_f}{m_e}+1+2\pi i\right)\right. \\
&- \left.\ln^2(1-r_3-r_4)+2\ln(1-r_3)\ln r_4+2\ln(1-r_4)\ln r_3\right\}. \qquad (2.39)
\end{aligned}$$

The result (2.37) gives the complete effect of FSR mass corrections neglecting terms suppressed by higher powers of $\frac{m_f^2}{s}$ as usual.

3 Differential Cross Section

This section translates our amplitudes into differential cross sections, and sets up comparisons with other related results. The initial state differential cross section for emitting one real photon may be written

$$\frac{d\sigma_1^{\mathrm{ISR}(0)}}{d^2\Omega dr_1 dr_2} = \frac{1}{2(4\pi)^4 s'}\sum_{\lambda_i,\sigma}\left|\mathcal{M}_1^{\mathrm{ISR}(0)}\right|^2\ , \qquad (3.1)$$

where the summed, squared real photon amplitude leads to

$$\left|\mathcal{M}_1^{\mathrm{ISR}(0)}\right|^2 = \frac{Q_e^4 e^6}{s^2 r_1 r_2}\left[(t_1^2+t_2^2)(F_0-F_1)+(u_1^2+u_2^2)(F_0+F_1)\right]\ , \qquad (3.2)$$

where the invariants u_i, t_i may be written in YFS3-style [2,17] effective angle notation:

$$\begin{aligned}
t_i &= (p_i-p_{i+2})^2 &&= -\frac{1}{4}\beta_f\beta_i s(1-r_i)[2-\cos(\theta_{1i})-\cos(\theta_{2i})] \\
u_i &= (p_i-p_{j+2})^2 &&= -\frac{1}{4}\beta_f\beta_i s(1-r_i)[2+\cos(\theta_{1i})+\cos(\theta_{2i})] \qquad (3.3)
\end{aligned}$$

with $(i,j)=(1,2)$ or $(2,1)$, and

$$\beta_f = \sqrt{1-\frac{4m_f^2}{s'}}, \qquad \beta_i = \sqrt{1-\frac{4m_e^2 s'}{s^2(1-r_i)^2}}. \qquad (3.4)$$

We will be setting these mass factors to unity in the following, and adding mass corrections at the end via (2.19) or (2.37).

The coefficients F_i are defined in terms of the standard vector and axial vector fermion couplings V and A, and $X=V^2+A^2$, $Y=2VA$ by

$$\begin{aligned}
F_0 &= X_e X_f \chi_2 + 2Q_e Q_f V_e V_f \chi_1 + Q_e^2 Q_f^2, \\
F_1 &= Y_e Y_f \chi_2 + 2Q_e Q_f A_e A_f \chi_1, \qquad (3.5)
\end{aligned}$$

where

$$\begin{aligned}\chi_1 &= s'(s'-M_Z^2)[(s'-M_Z^2)^2+(s'\Gamma_Z/M_Z)^2]^{-1}, \\ \chi_2 &= s'^2[(s'-M_Z^2)^2+(s'\Gamma_Z/M_Z)^2]^{-1}. \end{aligned} \tag{3.6}$$

The initial state differential cross section for real plus virtual photon emission may be expressed as

$$\frac{d\sigma_1^{\mathrm{ISR(1)}}}{d^2\Omega dr_1 dr_2} = \frac{1}{(4\pi)^4 s'} \sum_{\lambda_i,\sigma} \mathrm{Re}\left[(\mathcal{M}_1^{\mathrm{ISR(0)}})^* \mathcal{M}_1^{\mathrm{ISR(1)}}\right]. \tag{3.7}$$

If is convenient to rewrite (2.1) as

$$\mathcal{M}_1^{\mathrm{ISR(1)}} = \frac{Q_e^2 e^2}{16\pi^2}\, v\, \mathcal{M}_1^{\mathrm{ISR(0)}} \tag{3.8}$$

in terms of a virtual correction factor

$$v = f_0 + f_1 I_1 + f_2 I_2. \tag{3.9}$$

The differential cross section (3.7) can then be written in terms of a spin-averaged virtual correction factor $\langle v\rangle$ times the cross section for pure real initial state radiation:

$$d\sigma_1^{\mathrm{ISR(1)}} = \langle v\rangle\, d\sigma_1^{\mathrm{ISR(0)}}, \tag{3.10}$$

where

$$\begin{aligned}\langle v\rangle &= \frac{\sum_{\sigma,\lambda_1,\lambda_3} v\, |\mathcal{M}_1^{\mathrm{ISR(0)}}|^2}{\sum_{\sigma,\lambda_1,\lambda_3} |\mathcal{M}_1^{\mathrm{ISR(0)}}|^2} \\ &= \frac{\sum_{\lambda_1}\left\{v_+^{\lambda_1}[F_0+F_1+\lambda_1(F_2+F_3)] + v_-^{\lambda_1}[F_0-F_1+\lambda_1(F_2-F_3)]\right\}}{(F_0+F_1)(u_1^2+u_2^2)+(F_0-F_1)(t_1^2+t_2^2)}\end{aligned} \tag{3.11}$$

with

$$\begin{aligned}v_+^\lambda &= u_1^2 v_{\lambda,\lambda,-\lambda} + u_2^2 v_{\lambda,\lambda,\lambda}, \\ v_-^\lambda &= t_1^2 v_{\lambda,-\lambda,-\lambda} + t_2^2 v_{\lambda,-\lambda,\lambda},\end{aligned} \tag{3.12}$$

and

$$\begin{aligned}F_2 &= Y_e X_f \chi_2 + 2Q_e Q_f A_e V_f \chi_1, \qquad (3.13) \\ F_3 &= X_e Y_f \chi_2 + 2Q_e Q_f V_e A_f \chi_1.\end{aligned}$$

In the NLL approximation, where the f_1 and f_2 terms in (2.1) may be neglected, we may use the relation $\langle v \rangle = \langle f_0 \rangle$. Then (3.11) simplifies to

$$\begin{aligned}\langle f_0 \rangle &= 2\tfrac{(f_0(r_1,r_2)u_2^2+f_0(r_2,r_1)u_1^2)(F_0+F_1)+(f_0(r_1,r_2)t_2^2+f_0(r_2,r_1)t_1^2)(F_0-F_1)}{(u_1^2+u_2^2)(F_0+F_1)+(t_1^2+t_2^2)(F_0-F_1)} \\ &= \tfrac{F_0[\hat{f}_0(r_1,r_2)(1+\cos^2\theta_{11})+\hat{f}_0(r_2,r_1)(1+\cos^2\theta_{22})]+2F_1[\hat{f}_0(r_1,r_2)\cos\theta_{11}+\hat{f}_0(r_2,r_1)\cos\theta_{22}]}{F_0[(1-r_1)^2(1+\cos^2\theta_{11})+(1-r_2)^2(1+\cos^2\theta_{22})]+2F_1[(1-r_1)^2\cos\theta_{11}+(1-r_2)^2\cos\theta_{22}]} \qquad (3.14)\end{aligned}$$

with

$$\hat{f}_0(r_i, r_j) = 2(1-r_j)^2 f_0(r_i, r_j). \qquad (3.15)$$

If we further drop the dependence on θ_{ij} in (3.3), letting $\theta_{ij} \to \theta$ for fixed θ, then we get a simpler approximation. The angle dependence can be factored out of the cross-section (3.7), leading to

$$\frac{d\sigma_1^{\mathrm{ISR}(1)}}{dr_1 dr_2} = \frac{1}{2}\left(\frac{Q_e e^2}{2\pi^2}\right)^2 \sigma_0 \langle f_0 \rangle H_0(r_1, r_2). \qquad (3.16)$$

with the definition

$$H_0(r_1, r_2) = \frac{1}{2r_1 r_2}\left[(1-r_1)^2 + (1-r_2)^2\right], \qquad (3.17)$$

the total Born cross section

$$\sigma_0 = \frac{Q_e^2 Q_f^2 e^4}{2(4\pi)^2 s'} \int d^2\Omega \left(\frac{1}{2}F_0(1+\cos^2\theta) + F_1\cos\theta\right), \qquad (3.18)$$

and approximate spin-averaged form factor

$$\langle f_0 \rangle = \frac{(1-r_2)^2 f_0(r_1, r_2) + (1-r_1)^2 f_0(r_2, r_1)}{(1-r_1)^2 + (1-r_2)^2}. \qquad (3.19)$$

It can be shown that this approximation is valid to order NLL.

The NLL expression (2.18) then leads to the spin-averaged form factor

$$\begin{aligned}\langle f_0^{NLL} \rangle &= 2(L-1-i\pi) + 2\ln(1-r_1)(\ln r_2 + i\pi) + 2\ln(1-r_2)(\ln r_1 + i\pi) \\ &- \ln^2(1-r_1) - \ln^2(1-r_2) + 3\ln(1-r_1) + 3\ln(1-r_2) \\ &+ 2\mathrm{Sp}(r_1) + 2\mathrm{Sp}(r_2) + \frac{r_1(1-r_1)}{1+(1-r_1)^2} + \frac{r_2(1-r_2)}{1+(1-r_2)^2} \qquad (3.20)\end{aligned}$$

with mass corrections given by (2.19). This form is useful for comparison with other results on the differential cross section, as we will see in the next section.

An analogous expression can be found for the final state emission cross section. The spin-averaged version of the final state form factor (2.36) is

$$\begin{aligned}\overline{f}_0^{NLL} &= 4\pi\, B_{\mathrm{YFS}}(s', m_f) + 2(L-1-i\pi) - 2\ln r_3 \ln(1-r_4) \\ &- 2\ln r_4 \ln(1-r_3) - \ln(1-r_3) - \ln(1-r_4) - 2\mathrm{Sp}(r_3) - 2\mathrm{Sp}(r_4) \\ &- \frac{r_3}{1+(1-r_3)^2} - \frac{r_4}{1+(1-r_4)^2} \qquad (3.21)\end{aligned}$$

with mass corrections given by (2.37).

4 Partly Differential Cross Section and Comparisons

We may compare our spin-averaged initial state radiation form factor with one published in Ref. [5]. In our notation, this result may be written as

$$f_{IN} = \frac{\tilde{f}_{IN}(r_1,r_2) + \tilde{f}_{IN}(r_2,r_1)}{(1-r_1)^2 + (1-r_2)^2} \tag{4.1}$$

with

$$\begin{aligned} \tilde{f}_{IN}(r_1,r_2) &= (1-r_1-r_2+r_2^2)\left[4\pi \mathrm{Re}\, B_{\mathrm{YFS}}(s,m_e) + 2(L-1)\right] \\ &+ [1+(1-r_2)^2]\left\{\ln^2(r_1) + \ln^2\frac{1-r_1-r_2}{1-r_2} - \ln^2\frac{r_1}{1-r_1-r_2}\right. \\ &\qquad \left. + 2\,\mathrm{Sp}\left(\frac{1-r_1-r_2}{1-r_2}\right) + 2\,\mathrm{Sp}(r_1+r_2) - \frac{\pi^2}{3}\right\} \\ &+ \frac{r_1 r_2(1-r_1-r_2)}{1-r_2}\left(\frac{1}{1-r_2} + 1 - \frac{3r_2}{r_1}\right)\ln\frac{r_1}{1-r_1-r_2} \\ &- \frac{2r_1r_2(1-r_1-r_2)}{r_1+r_2}\left(\frac{(1-r_1-r_2)}{r_1+r_2} - \frac{3}{r_1}\right)\ln(1-r_1-r_2) \\ &+ r_2(3r_2+2r_1)\ln(r_1) - \frac{2r_1r_2}{r_1+r_2} + \frac{r_1r_2}{1-r_2} + r_2(1-r_2). \end{aligned} \tag{4.2}$$

The NLL limit of this expression may be obtained by summing the two collinear limits where $r_i \to 0$ separately. Carrying this out leads precisely to our spin-averaged NLL expression (3.20). Thus, we agree with Ref. [5] to NLL order. Note that the expression f_{IN} does not include mass corrections, which were not calculated in Ref. [5].

By integrating out the separate dependence on r_i in favor of the variable $z = s'/s = 1 - r_1 - r_2$, we may obtain a result which can be compared to Ref. [4]. To begin, we consider the pure real photon ISR cross section, and work in the approximation where the effective angles θ_{ij} in (3.3) are replaced by a common angle θ. Then

$$\frac{d\sigma_1^{\mathrm{ISR}(0)}}{dr_1 dr_2} = \frac{Q_e^2 e^2}{4\pi^2}\sigma_0 H_0(r_1,r_2) \tag{4.3}$$

in terms of H_0 defined by (3.17). Integrating r_1 and r_2 with the constraint $z = 1 - r_1 - r_2$ gives

$$\frac{d\sigma_1^{\mathrm{ISR}(0)}}{dz} = \frac{Q_e^2 e^2}{4\pi^2}\sigma_0 \int_{r_0}^{1-z-r_0} dr_1 dr_2 \delta(1-z-r_1-r_2) H_0(r_1,r_2), \tag{4.4}$$

where $r_0 = m_e^2(1-z)/s$ is the kinematic minimum value of r_1 or r_2. The result of the integral is, exactly,

$$\frac{d\sigma_1^{\mathrm{ISR}(0)}}{dz} = \frac{Q_e^2 e^2}{4\pi^2}\sigma_0 \left(\frac{1+z^2}{1-z}\right)\left[L - \frac{(1-z)^2}{1+z^2}\right]. \tag{4.5}$$

Mass corrections, obtained by the prescription of Ref. [16], have the effect of replacing H_0 by $H_0 + H_m$ in (4.3), where

$$H_m(r_1, r_2) = -\frac{2m_e^2}{s}\left(\frac{r_1}{r_2} + \frac{r_2}{r_1}\right)\frac{z}{1+z^2} H_0(r_1, r_2). \tag{4.6}$$

Integrating the mass term gives

$$\int_{r_0}^{1-z-r_0} dr_1 dr_2 H_m(r_1, r_2) = -\frac{2z}{1-z} + \mathcal{O}(\frac{m_e^2}{s}). \tag{4.7}$$

The total mass-corrected real photon emission cross section is then

$$\frac{d\sigma_1^{\mathrm{ISR}(0)}}{dz} = \frac{Q_e^2 e^2}{4\pi^2}\sigma_0\left(\frac{1+z^2}{1-z}\right)(L-1) = \delta_1^{H_1}(z)\sigma_0. \tag{4.8}$$

in the notation of Ref. [4], where this result matches the real part of (2.11).

The real plus virtual ISR cross section is

$$\frac{d\sigma_1^{\mathrm{ISR}(1)}}{dz} = \frac{1}{2}\left(\frac{Q_e e^2}{4\pi^2}\right)^2 \sigma_0 \int_{r_0}^{1-z-r_0} dr_1 dr_2 \delta(1-z-r_1-r_2)\langle f_0 \rangle H_0(r_1, r_2), \tag{4.9}$$

where we use the NLL expression (3.20) for the virtual form factor, and will add mass corrections later. Doing the integral and keeping all infrared terms and terms of order L^2 and L gives

$$\begin{aligned}\frac{d\sigma_1^{\mathrm{ISR}(1)}}{dz} &= \frac{Q_e^2 e^2}{4\pi^2}\sigma_0 \delta_1^{V_1}(s)\left(\frac{1+z^2}{1-z}\right)\left[L - \frac{(1-z)^2}{1+z^2}\right] \\ &+ \frac{1}{2}\left(\frac{Q_e^2 e^2}{4\pi^2}\right)^2 \sigma_0 L \left(\frac{1+z^2}{1-z}\right)\Big\{ - L\ln z + 2\ln z \ln(1-z) \\ &+ 2\,\mathrm{Sp}(1-z) + 3\ln z - \ln^2 z + \frac{z(1-z)}{1+z^2}\Big\},\end{aligned} \tag{4.10}$$

where we use the notation of Ref. [4] for

$$\delta_1^{V_1}(s) = \frac{Q_e^2 e^2}{4\pi^2}\left\{2\pi B_{\mathrm{YFS}}(s, m_e) + L - 1\right\}. \tag{4.11}$$

The mass correction is obtained by multiplying the pure real mass correction by the single virtual photon form factor evaluated in terms of s' rather than s. Thus, we add to the differential cross section a mass term

$$\frac{d\sigma_m}{dr_1 dr_2} = \frac{Q_e^2 e^2}{4\pi^2}\delta_1^{V_1}(s') H_m(r_1, r_2)\ \sigma_0, \tag{4.12}$$

where

$$\begin{aligned}\delta_1^{V_1}(s') &= \frac{Q_e^2 e^2}{4\pi^2}\left\{2\pi B_{\rm YFS}(s',m_e) + L + \ln z - 1\right\} \\ &= \delta_1^{V_1}(s) + \left(\frac{Q_e e^2}{4\pi^2}\right)\ln z\left(2\ln\frac{m_0}{m_e} - L + \frac{3}{2} - \ln^2 z\right). \end{aligned} \qquad (4.13)$$

Integrating over r_1 and r_2 with $z = 1 - r_1 - r_2$ and keeping only infrared terms and terms of order L, we obtain

$$\frac{d\sigma_m}{dz} = -\frac{Q_e^2 e^2}{4\pi^2}\frac{2z}{1-z}\sigma_0\Big\{\delta_1^{V_1}(s) - \frac{Q_e^2 e^2}{4\pi^2}L\ln z\Big\}. \qquad (4.14)$$

Adding the mass corrections and using the notation of (4.8) gives the complete real plus virtual cross section at order NLL,

$$\begin{aligned}\frac{d\sigma_1^{\rm ISR(1)}}{dz} &= \sigma_0\delta_1^{V_1}(s)\delta_1^{H_1} + \tfrac{1}{2}\left(\tfrac{Q_e^2 e^2}{4\pi^2}\right)^2\sigma_0 L\Big\{\left(\tfrac{4z}{1-z}\right)\ln z + z \\ &+ \left(\tfrac{1+z^2}{1-z}\right)\left[-L\ln z + 2\ln z\ln(1-z) + 3\ln z - \ln^2 z + 2\,{\rm Sp}(1-z)\right]\Big\}\ . \end{aligned} \qquad (4.15)$$

This result agrees precisely with the terms in (2.26) of Ref. [4] through order $\alpha^2 L$.

We illustrate the agreement we have found above in Figs. 2-5, for the case $f\bar{f} = \mu^-\mu^+$. In Fig. 2, we show the complete $\beta_1^{(2)}$ distribution for our exact result, our NLL and LL approximate results, the result of Igarashi and Nakazawa *et al.* [5], and the result of Berends *et al.* [4]. What we see is that there is a very good general agreement between all of these results. To better assess the difference between them, we plot in Fig. 3 the difference between the respective $\mathcal{O}(\alpha^2)$ and $\mathcal{O}(\alpha^1)$ results. Again we see very good agreement except for the hardest possible photons, where then the LL result differs significantly from the others.

To isolate the respective predictions for the NLL effect, we plot in Fig. 4 the respective differences between our LL $\mathcal{O}(\alpha^2)$ result and the other four results. We see that there is again very good agreement but, at the level of $0.5\cdot 10^{-4}$, the result of Ref. [4] is somewhat smaller in magnitude than the other three NLL results in the Z radiative return regime above a cut of 0.75.

Finally, in the Fig. 5 we isolate the size of the three NNLL results by plotting the difference between our NLL result and our exact result, the result from Ref. [5] and the result from Ref. [4]. We again see that the most pronounced difference in the results occurs for the regime above $v_{max} = 0.75$ where the result of Ref. [4] differs by $0.5\cdot 10^{-4}$ from the other two for $v_{max} < 0.975$ and differs from the exact result by $1.5\cdot 10^{-4}$ for $v_{max} > 0.975$. The result from Ref. [5] differs from the exact result by $0.2\cdot 10^{-4}$ for $v_{max} > 0.975$ but is essentially indistinguishable from it for smaller values of v_{max}. We

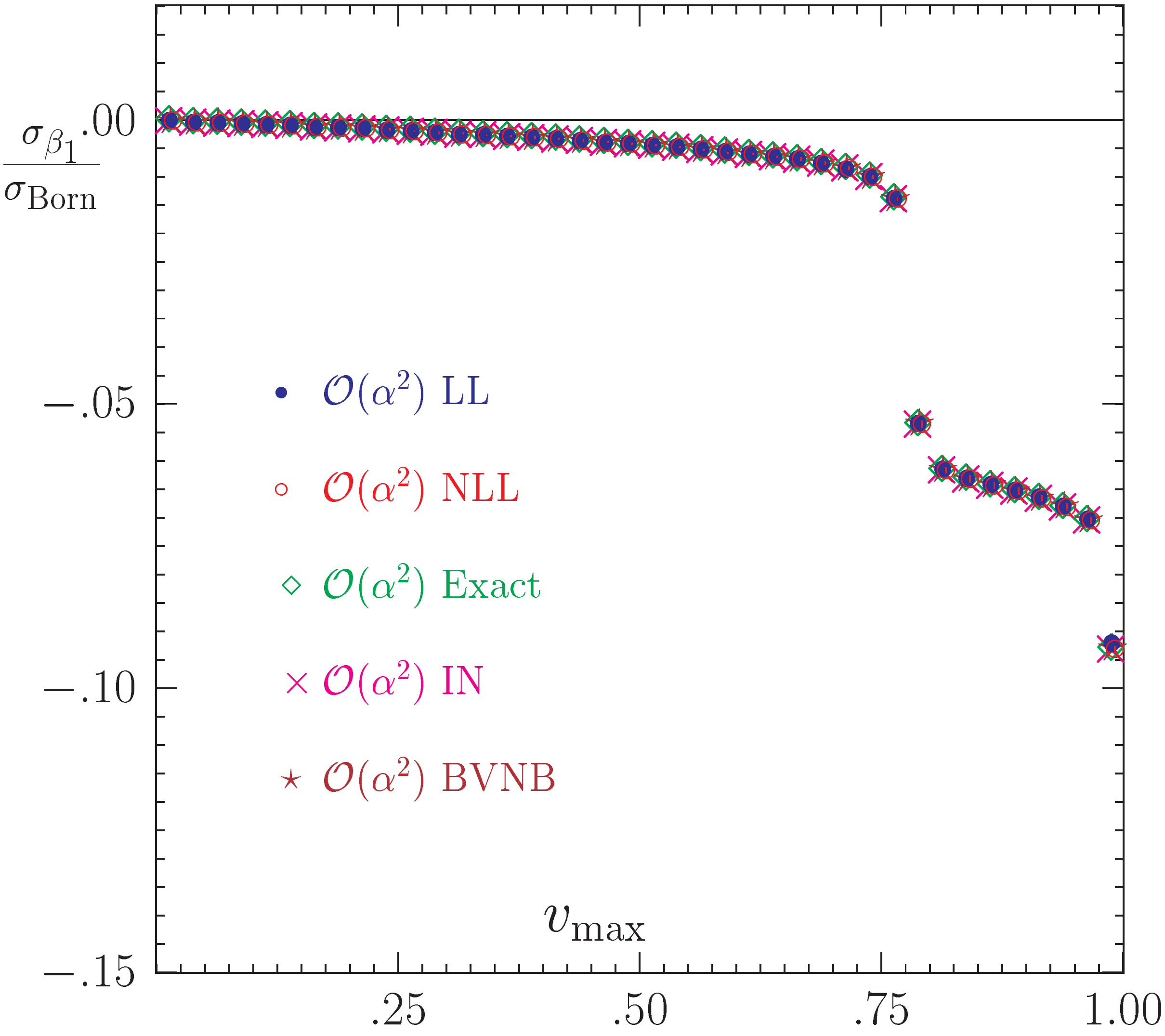

Figure 2: This is the $\beta_1^{(2)}$ distribution for the YFS3ff MC (YFS3ff is the EEX3 matrix element option of the $\mathcal{KK}$ MC in Ref. [2]), as a function of energy cut $v_{\max}$. It is divided by the Born cross-section. The IN result is from Ref. [5], and the BVNB result is from Ref. [4].

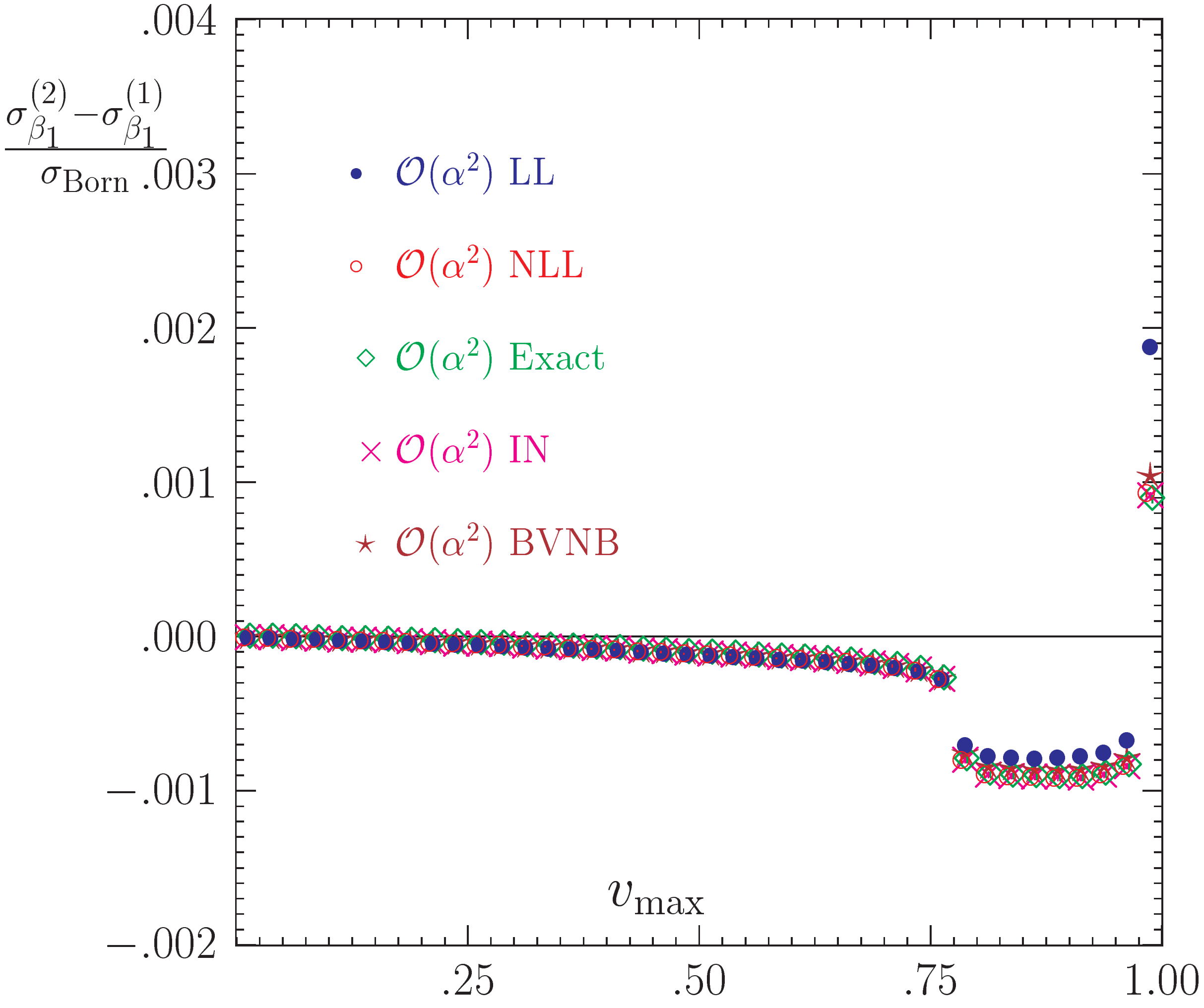

Figure 3: Difference $\beta_1^{(2)} - \beta_1^{(1)}$ for the YFS3ff MC (the EEX3 option in the $\mathcal{KK}$ MC), as a function of the cut $v_{\rm max}$. It is divided by the Born cross-section.

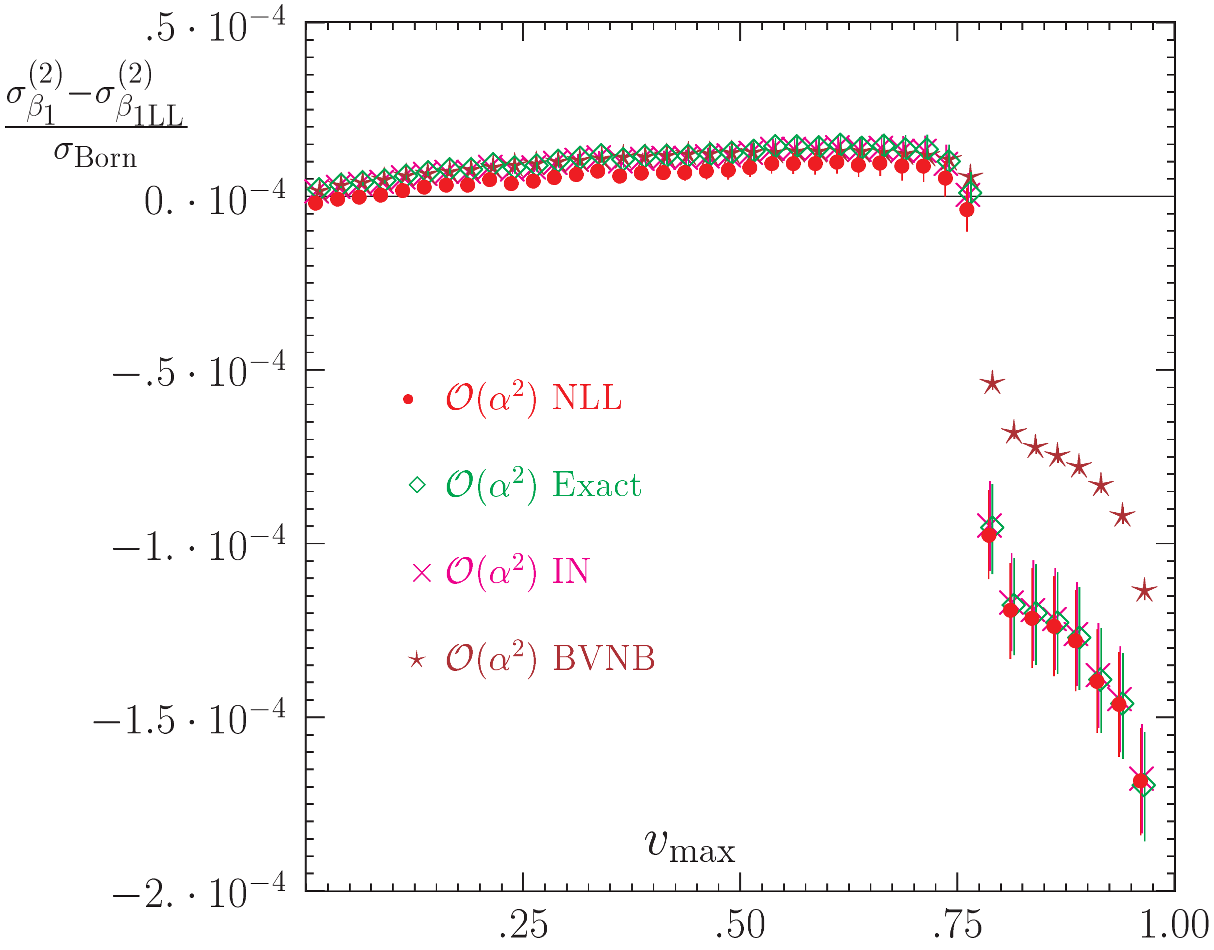

Figure 4: Next-to-leading-log contribution $\beta_1^{(2)} - \beta_{1LL}^{(2)}$ for the YFS3ff MC (the EEX3 option of the $\mathcal{KK}$ MC), as a function of the cut $v_{\rm max}$. It is divided by the Born cross-section.

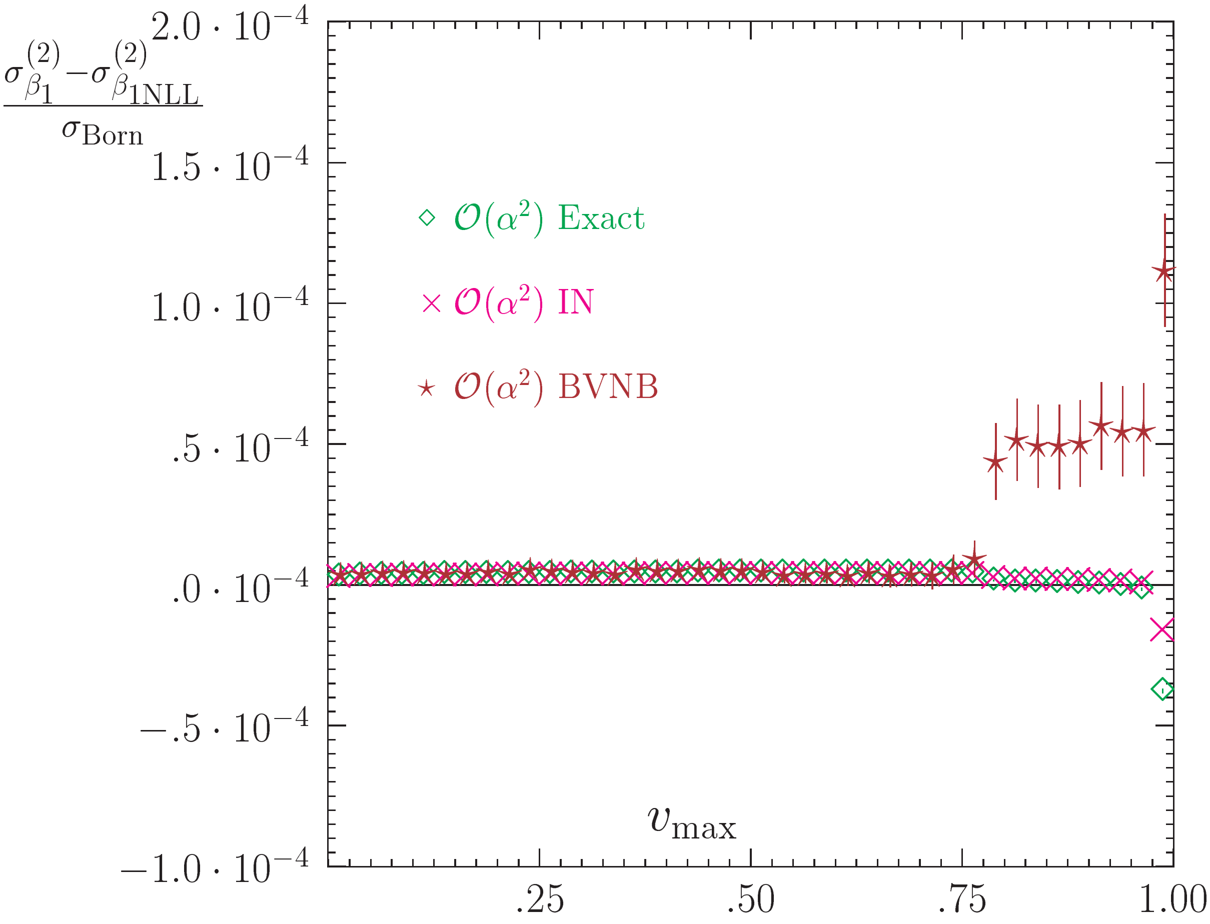

Figure 5: Sub-NLL contribution $\beta_1^{(2)} - \beta_{1\mathrm{NLL}}^{(2)}$ for the YFS3ff MC (the EEX3 option of the $\mathcal{KK}$ MC), as a function of the cut $v_{\max}$. It is divided by the Born cross-section.

conclude that our exact result for the $\mathcal{O}(\alpha^2)$ correction $\bar{\beta}_1^{(2)}$ has a total precision tag of $1.5 \cdot 10^{-4}$. Its NLL effect has already been implemented in the $\mathcal{KK}$ MC in Ref. [2].

We have also made the analogous study to Figs. 2-5 for 500 GeV. We find very similar results, with the total precision tag of $2 \cdot 10^{-4}$.

5 Conclusions

In this paper, we have presented exact results for the virtual correction to the process $e^+e^- \to f\bar{f} + \gamma$ for the $ISR \oplus FSR$. The results are already in use in the $\mathcal{KK}$ MC in Ref. [2] in connection with the final LEP2 data analysis.

We have compared our results with those in Refs. [4, 5] and in general we find very good agreement, both at 200 GeV and at 500 GeV. For example, the size of the NNLL correction is shown to be at or below the level of $2 \cdot 10^{-4}$ for all values of the energy cut parameter. Our results are fully differential and are therefore ideally suited for MC event generator implementation. This has been done in the $\mathcal{KK}$ MC in Ref. [2]. To compare our results with the results in Refs. [4], we have partially integrated them accordingly. While the results in Ref. [5] are also fully differential, they lack the complete mass corrections that our results do have. In this way, one sees that our results are in fact unique. They are an important part of the complete $\mathcal{O}(\alpha^2)$ corrections to the $2f$ production process needed for precision studies of such processes in the final LEP2 data analysis and in the future TESLA/LC physics.

Acknowledgments

Two of the authors (S.J. and B.F.L.W.) would like to thank Prof. G. Altarelli of the CERN TH Div. and Prof. D. Schlatter and the ALEPH, DELPHI, L3 and OPAL Collaborations, respectively, for their support and hospitality while this work was completed. B.F.L.W. would like to thank Prof. C. Prescott of Group A at SLAC for his kind hospitality while this work was in its developmental stages.

Note Added

After we had submitted this paper, we became aware of related work by G. Rodrigo, A. Gehrmann-De Ridder, M. Guilleaume and J. H. Kuhn, hep-ph/0106132. These authors also agree with the analogous results of Ref. [4], when the photon azimuthal angle is integrated and the photon polarization is summed for the ISR process.

A Scalar Integrals

Previously, in Ref. [10], the analogous exact virtually corrected photon cross sections were expressed in the t channel using scalar integral functions which were calculated by a numerical package FF described in Ref. [15]. In the present paper, we have expressed these functions directly in terms of logarithms and dilogarithms. This appendix will give the expressions for the individual scalar integrals in the s channel.

The notation for the scalar integrals will match Ref. [10], with kinematic notation defined in Sections 1 and 2 of this paper. The scalar integrals with two denominators are denoted B, and the ones appearing in the form factors are

$$\begin{aligned}
B_{12} &= B(m_e^2; m_\gamma, m_e), \\
B_{13}^{r_i} &= B(m_e^2 - sr_i; m_\gamma, m_e), \\
B_{23} &= B(m_\gamma^2; m_e, m_e), \\
B_{24} &= B(s; m_e, m_e), \\
B_{34} &= B(s'; m_e, m_e),
\end{aligned} \tag{A.1}$$

where the first argument is the square of the momentum through the diagram, and the remaining arguments are the masses of the two lines. These functions are UV divergent, but only the following finite combinations are needed:

$$B_{13}^{r_i} - B_{34} = \ln\frac{s'}{sr_i} + \frac{m_e^2}{m_e^2 - sr_i}\ln\frac{sr_i}{m_e^2} - i\pi, \tag{A.2}$$

$$B_{24} - B_{34} = \ln\frac{s'}{s}, \tag{A.3}$$

$$B_{12} - B_{34} = \ln\frac{s'}{m_e^2} - i\pi. \tag{A.4}$$

The mass term in (A.2) has been dropped when applying this expression, since the mass corrections are added explicitly to the massless limit of the calculation using the prescription of Ref. [16].

The integrals for three and four denominators are obtained from the appendix of Ref. [5]. For three denominators, we need the expressions

$$\begin{aligned}
C_{123}^{r_i} &= C(m_e^2, m_\gamma^2, m_e^2 - sr_i; m_\gamma, m_e, m_e), \\
C_{134}^{r_i} &= C(m_e^2 - sr_i, s', m_e^2; m_\gamma, m_e, m_e), \\
C_{234} &= C(m_\gamma^2, s', s; m_e, m_e, m_e), \\
C_{124} &= C(m_e^2, s, m_e^2; m_\gamma, m_e, m_e),
\end{aligned}$$

where the first three arguments are the squares of the external momenta, and the next three are the masses of the three lines, in cyclic order. The results are

$$\begin{aligned}
s r_i C_{123}^{r_i} &= -\frac{1}{2}\ln^2\frac{m_e^2}{s r_i} - \mathrm{Sp}\left(1-\frac{m_e^2}{s r_i}\right) - \frac{\pi^2}{6}, && \text{(A.5)}\\
(1-r_j)s\, C_{134}^{r_i} &= \frac{1}{2}\ln^2\frac{s'}{m_e^2} - \frac{1}{2}\ln^2\frac{(1-r_j)s}{m_e^2} - \frac{1}{2}\ln^2\frac{1-r_j}{r_i} \\
&+ 2\ln\frac{s'}{m_e^2}\ln\left(\frac{1-r_j}{r_i}\right) + \ln\frac{m_e^2}{s r_i}\ln\left(\frac{1-r_j}{r_i}\right) - \mathrm{Sp}\left(\frac{m_e^2}{s r_i}\right) \\
&- 2\mathrm{Sp}\left(\frac{s'}{s(1-r_j)}\right) - \frac{5\pi^2}{6} - \pi i\ln\frac{s'}{m_e^2} - 2\pi i\ln\left(\frac{1-r_j}{r_i}\right), && \text{(A.6)}\\
(r_1+r_2)s\, C_{234} &= \frac{1}{2}\ln^2\frac{s}{m_e^2} - \frac{1}{2}\ln^2\frac{s'}{m_e^2} + \pi i\ln\frac{s'}{s}, && \text{(A.7)}\\
s C_{124} &= \frac{1}{2}\ln^2\frac{s}{m_e^2} - \ln\frac{s}{m_e^2}\ln\frac{m_\gamma^2}{m_e^2} - \frac{2\pi^2}{3} + \pi i\ln\frac{m_\gamma^2}{s}. && \text{(A.8)}
\end{aligned}$$

The expression (A.5) is an analytic continuation of the one in Ref. [5], as required since $r_i < m_e^2$ is possible, and the expression (A.6) drops mass terms. In particular, the photon mass regulator m_γ is dropped whenever possible.

The expression with four denominators is

$$\begin{aligned}
s^2 r_i D_{1234}^{r_i} &= \ln^2\frac{s'}{m_e^2} - 2\ln\frac{s}{m_e^2}\ln\frac{s r_i}{m_e^2} + \ln\frac{m_\gamma^2}{m_e^2}\left(\ln\frac{s}{m_e^2} - i\pi\right) \\
&+ 2\,\mathrm{Sp}(r_1+r_2) - \frac{5\pi^2}{6} - 2\pi i\ln\frac{s'}{s r_i}. && \text{(A.9)}
\end{aligned}$$

All of these expressions have been checked for agreement with the FF package. The function R defined in equations (2.13) and (2.14) and appearing in the virtual photon factors is the IR-finite combination

$$R(r_i, r_j) = s\,(C_{124} + s r_j D_{1234}^{r_j}) - s r_j C_{123}^{r_j} - (1-r_i)s\, C_{134}^{r_j} + (r_1+r_2)s\, C_{234}. \qquad \text{(A.10)}$$

This completes the appendix.

References

[1] M. Kobel *et al.*, hep-ph/0007180, in *Reports of the working groups on precision calculations for LEP2 physics*, CERN-2000-09, eds. S. Jadach, G. Passarino and R. Pittau, (CERN, Geneva, 2000) p. 269.

[2] S. Jadach, B.F.L. Ward and Z. Wąs, *Phys. Rev.* **D63** (2001) 113009; *Comput. Phys. Commun.* **130** (2000) 260; and references therein.

[3] D. Bardin *et al.*, *Comput. Phys. Commun.* **133** (2001) 229.

[4] F.A. Berends, W.L. Van Neerven and G.J.H. Burgers, *Nucl. Phys.* **B297** (1988) 429 and references therein.

[5] M. Igarashi and N. Nakazawa, *Nucl. Phys.* **B288** (1987) 301.

[6] S. Jadach, B.F.L. Ward, and Z. Wąs, "Global positioning of spin GPS scheme for half-spin massive spinors", 1998, preprint hep-ph/9905452, CERN-TH/98-235, submitted to *Eur. J. Phys. C.*

[7] S. Jadach, B.F.L. Ward and Z. Wąs, *Phys. Lett* **B449** (1999) 97.

[8] R. Kleiss and W.J. Stirling, Nucl.Phys. **B262** (1985) 235; Phys. Lett. B**179** (1986) 159.

[9] J.A.M. Vermaseren, The symbolic manipulation program FORM, versions 1-3, available via anonymous FTP from nikhefh.nikhef.nl.

[10] S. Jadach, M. Melles, B.F.L. Ward and S.A. Yost, *Phys. Lett.* **B377** (1996) 168.

[11] A. Arbuzov *et al.*, *Phys. Lett.* **B383** (1996) 238; S. Jadach, M. Melles, B.F.L. Ward and S.A. Yost, *Phys. Lett.* **B450** (1999) 262.

[12] S. Jadach, W. Placzek, E. Richter-Wąs, B.F.L. Ward and Z. Wąs, *Comput. Phys. Commun.* **102** (1997) 229.

[13] J.D. Bjorken and S.D. Drell, *Relativistic Quantum Fields*, (McGraw-Hill, Menlo Park, 1965).

[14] Z. Xu, D.-H. Zhang and L. Chang, *Nucl. Phys.* **B291** (1987), 392.

[15] G.J. van Oldenborgh and J.A.M. Vermaseren, *Zeit. Phys.* **C46** (1990), 425.

[16] F.A. Berends, P. De Causmaecker, R. Gastmans, R. Kleiss, W. Troost and T.T. Wu, *Nucl. Phys.* **B264** (1986) 243, 265.

[17] S. Jadach and B.F.L. Ward, Phys. Lett. **B274** (1992) 470. The YFS3 matrix element is the EEX3 calculation in Ref. [2].

Figure Captions

Fig. 1. Initial state radiation graphs for $e^+e^- \to f\overline{f}$ with one virtual and one real photon, for $f \neq e$.

Fig. 2. This is the $\beta_1^{(2)}$ distribution for the YFS3ff MC (YFS3ff is the EEX3 matrix element option of the $\mathcal{KK}$ MC in Ref. [2]), as a function of energy cut $v_{\rm max}$. It is divided by the Born cross-section.

Fig. 3. Difference $\beta_1^{(2)} - \beta_1^{(1)}$ for the YFS3ff MC (the EEX3 option in the $\mathcal{KK}$ MC), as a function of the cut $v_{\rm max}$. It is divided by the Born cross-section.

Fig. 4. Next-to-leading-log contribution $\beta_1^{(2)} - \beta_{1\rm LL}^{(2)}$ for the YFS3ff MC (the EEX3 option of the $\mathcal{KK}$ MC), as a function of the cut $v_{\rm max}$. It is divided by the Born cross-section.

Fig. 5. Sub-NLL contribution $\beta_1^{(2)} - \beta_{1\rm NLL}^{(2)}$ for the YFS3ff MC (the EEX3 option of the $\mathcal{KK}$ MC), as a function of the cut $v_{\rm max}$. It is divided by the Born cross-section.